Novel Action of Paclitaxel against Cancer Cells: Bystander Effect Mediated by Reactive Oxygen Species

Jérôme Alexandre,[1,3] Yumin Hu,[1,2] Weiqin Lu,[1,2] Helene Pelicano,[1] and Peng Huang[1,2]

[1]Department of Molecular Pathology, The University of Texas M. D. Anderson Cancer Center; [2]Graduate School of Biomedical Sciences, The University of Texas at Houston, Houston, Texas; and [3]Université Paris-Descartes, Faculté de Médecine, Assistance Publique-Hôpitaux de Paris, France

Abstract

Generation of reactive oxygen species (ROS) has been observed in cancer cells treated with paclitaxel, but the underlying mechanisms and therapeutic implications remain unclear. In the present study, we showed that paclitaxel promoted ROS generation through enhancing the activity of NADPH oxidase (NOX) associated with plasma membranes. Treatment of breast cancer cells caused an increased translocation of Rac1, a positive regulatory protein of NOX, to the membrane fraction. The paclitaxel-induced ROS generation occurred rapidly within several hours of drug exposure, with O_2^- and H_2O_2 accumulation mainly outside the cells while the intracellular ROS remained unchanged. Importantly, the increase in extracellular ROS caused lethal damage to the bystander cancer cells not exposed to paclitaxel, as shown by two different methods using coculture systems where the bystander cells were differentiated from the paclitaxel-treated cells by fluorescent or radioactive labeling. This cytotoxic bystander effect was also observed with other microtubule-targeted agents vincristine and taxotere but not with 5-fluorouracil or doxorubicin. This toxic bystander effect was enhanced by CuZnSOD that converts O_2^- to H_2O_2 and was abolished by a catalase that eliminates H_2O_2. Furthermore, paclitaxel was able to induce an almost complete inhibition of proliferation of the bystander cells in the coculture system. Our study revealed a novel mechanism by which paclitaxel induces toxic bystander effect through generation of extracellular H_2O_2 from the membrane-associated NOX. This may contribute to the potent anticancer activity of paclitaxel and provide a novel basis to improve the clinical use of this important drug. [Cancer Res 2007;67(8):3512–17]

Introduction

Paclitaxel is a microtubule-targeted agent widely used in cancer therapy. Its primary cellular effect is to cause abnormal stabilization of the dynamic microtubule polymerization, leading to the failure of mitosis. In addition, paclitaxel also alters other cellular functions that involve microtubules, such as intracellular signaling and organelle transport and locomotion (1). Recent studies showed that paclitaxel is able to induce early reactive oxygen species (ROS) production in cancer cells, and hydrogen peroxide (H_2O_2) was found to be involved in paclitaxel-induced cancer cell death *in vitro* and *in vivo* (2–4). However, the mechanisms of paclitaxel-induced oxidative stress remain unknown. H_2O_2 mainly comes from the dismutation of superoxide (O_2^-), a reaction catalyzed by superoxide dismutases (SOD). Most cellular O_2^- is produced by mitochondrial respiratory chain as a product of aerobic metabolism (5). Another significant source of O_2^- is NADPH oxidases (NOX), which are mainly associated with plasma membrane and produce O_2^- outside the cells (6). NOX activity is regulated by the assembling of active enzyme complex from catalytic subunits $gp91^{phox}$, $p22^{phox}$, and Rac1 and other components. The translocation of Rac1 from cytosol to the plasma membrane seems to be a crucial step in NOX activation and O_2^- production (7). The objectives of the present study were to determine the source or subcellular location of the ROS production induced by paclitaxel and to evaluate the possible contribution of ROS in mediating its cytotoxic effect.

Materials and Methods

Materials and cell culture. Dihydroethidine, *N*-acetyl-3,7-dihydroxyphenoxazine, and 5-chloromethylfluoroscein diacetate (CMFDA) were purchased from Molecular Probe (Eugene, OR), and ^{3}H-thymidine was purchased from Amersham (Piscataway, NJ). Mouse anti-Rac1, mouse anti-β-actin, and rabbit anti-$p22^{phox}$ antibodies were from BD Biosciences (San Diego, CA), Sigma (St. Louis, MO), and Santa Cruz Biotechnology (Santa Cruz, CA), respectively. Human breast cancer cell line MCF7 was cultured in a 1:1 mix of DMEM and F12 medium. Human lung cancer cell line H1299, human leukemia cell line HL-60, and the mitochondrial respiratory-defective HL60/C6F clone were cultured in RPMI 1640. All media were supplemented with 10% fetal bovine serum (FBS). The HL60/C6F cell culture medium was also supplemented with 1 mmol/L sodium pyruvate, 50 μmol/L uridine, and an additional 2.7% glucose.

Assays of ROS production. Intracellular O_2^- was measured by flow cytometry using dihydroethidine as described (5). SOD-inhibitable reduction of cytochrome *c* was used to detect extracellular O_2^- release as previously described (8). Briefly, MCF7 cells in 96-well plates at 80% confluence were incubated with 100 nmol/L paclitaxel for 1 h in Hank's buffer saline (HBS). Cytochrome *c* (110 μmol/L) and catalase (70 units/mL) were then added, with or without 100 units/mL CuZnSOD. Absorbance was measured at 550 nm after a 20-min incubation. The A_{550} values were converted to nanomoles of cytochrome *c* reduced, using a net extinction coefficient of 2.1×10^4 $(mol/L)^{-1}$ cm^{-1}. O_2^- concentration was calculated from the difference in the amounts of cytochrome *c* reduced in the absence and presence of CuZnSOD. Extracellular H_2O_2 was determined by fluorometry in 96-well plates using *N*-acetyl-3,7-dihydroxyphenoxazine as a cell-impermeable probe as previously described (9). The cells were incubated with 100 nmol/L paclitaxel, 50 μmol/L Amplex red, and 0.1 units/mL horseradish peroxidase in serum-free medium for 60 min at 37°C. Fluorescence was measured using excitation at 530 nm and detection at 590 nm. Because this assay has a high fluorescent background, samples containing the same medium and Amplex red reagents without cells were run in parallel as blank control for subtraction of the nonspecific fluorescent background from the test samples. The net values were then used to calculate extracellular H_2O_2 concentrations using a H_2O_2 standard curve determined under the same conditions.

Requests for reprints: Peng Huang, Department of Molecular Pathology, The University of Texas M. D. Anderson Cancer Center, Unit 951, Houston, TX 77054. Phone: 713-792-7742; Fax: 713-794-4672; E-mail: phuang@mdanderson.org.

doi:10.1158/0008-5472.CAN-06-3914

Assay of NOX activity associated with cell membranes. Cells were scraped and suspended in ice-cold buffer containing 20 mmol/L HEPES, 10 mmol/L KCl, 1.5 mmol/L $MgCl_2$, 1 mmol/L EDTA, 1 mmol/L EGTA, 100 mmol/L sucrose, and a cocktail of protease inhibitors. The cell suspension was homogenized with 15 strokes in a glass tissue homogenizer. The samples were centrifuged at 800× *g* at 4°C for 5 min to remove unbroken cells and nuclei. The supernatants were centrifuged again at 100,000 × *g* for 30 min to separate the membrane fraction (pellet) and the cytosolic fraction (supernatant) as described (10). Protein concentrations were determined using a BCA Protein Assay kit (Pierce, Rockford, IL) with bovine serum albumin as standard. Generation of O_2^- in the membrane fraction was measured by lucigenin chemoluminescence in 100 μL of HBS containing 100 μmol/L NADPH, 50 μmol/L lucigenin, and 1.75 μg of cell membrane proteins (11). After a 5-min incubation at 37°C, chemiluminescence was measured using a luminometer (Turner Designs, Sunnyvale, CA) for 1 min. The signal was normalized and expressed as arbitrary light units per microgram protein per minute.

Immunoblotting of membrane-associated proteins. Cell membrane fractions were isolated as described above, and the associated proteins (20 μg) were resolved by electrophoresis on 12% SDS-PAGE and transferred to nitrocellulose membranes. The membranes were blotted for molecules of interest with anti-Rac1 (1:2,000), anti-$p22^{phox}$ (1:500), and anti-actin (1:10,000) antibodies overnight. The bound primary antibodies were detected using proper horseradish peroxidase–conjugated secondary antibodies followed by detection with a SuperSignal enhanced chemiluminescence kit (Pierce). For sequential blotting, the membranes were stripped with a stripping buffer (Pierce) followed by reblotting with proper antibodies.

Assessment of cytotoxic bystander effect using fluorescent probes. For cell labeling, we used a fluorescent probe CMFDA, which passes cell membranes freely. Once inside the cells, it is converted to cell-impermeable green fluorescent product. After loading, cells remain fluorescent for several days and proliferate for at least four cell divisions (12). MCF7 cells were first incubated with 5 μmol/L CMFDA at 37°C for 30 min in serum-free medium, which was then replaced by fresh medium (with 10% FBS without CMFDA) for another 30 min before the cells were trypsinized for coculture with unlabeled MCF7 cells pretreated with 100 nmol/L paclitaxel for 3 h in six-well plates (50% confluence). Paclitaxel was removed by extensive washing with fresh medium, and the CMFDA-labeled cells in fresh medium were added to each well in the presence or absence of catalase or SOD as indicated. As a negative control, CMFDA-labeled cells were cocultured with untreated MCF7 cells. The ratio of CMFDA-labeled cells to unlabeled drug-treated cells was ~1:3. After 48 h of coculture, cell death was assessed by direct propidium iodide (PI) staining (1 μg/mL PI in 1 mL PBS per well). The dead cells with compromised membrane integrity became permeable to PI, and their nuclei appeared either red (paclitaxel treated) or yellow (CMFDA-labeled cells, indicative of bystander effect). Cell images were captured using a Nikon fluorescent microscope (Eclipse TE300). To evaluate the ROS effect on the growth of bystander cells, the number of CMFDA-labeled cells was directly counted in 24-well plate under fluorescent microscope 4 h after plating (baseline cell number) and 48 h after coculture. In each well, cells were counted in three separate areas of 0.4 mm^2 per field. Each condition was done in triplicate. Thus, the cell density was calculated as the mean of nine separate measurements.

Measurement of toxic bystander effect by ^{3}H-thymidine labeling. MCF7 cells (5×10^4 per mL) were incubated with 2 μCi/mL ^{3}H-thymidine for 48 h, washed twice with PBS, and trypsinized for coculture with unlabeled MCF7 cells (50% confluence) pretreated for 3 h with paclitaxel (50–500 nmol/L), taxotere (100–500 nmol/L), vincristine (300 nmol/L), 5-fluorouracil (5-FU; 1 mmol/L), and doxorubicin (3 μmol/L) in a similar fashion as described above. Nonadherent cells were removed after overnight incubation. After a 96-h coculture, radioactivity in the culture medium released from the bystander cells was measured using a scintillation counter. The level of radioactivity in the medium was indicative of cell death from the ^{3}H-thymidine–labeled population (13).

Statistical analysis. Student's *t* test was used to evaluate the statistical differences of the experimental values between two samples to be compared.

Results and Discussion

Paclitaxel induces NOX activation and extracellular release of O_2^- and H_2O_2. We first examined the effect of paclitaxel on intracellular ROS levels in MCF7 cells. As shown in Fig. 1*A*, exposure of cells to a toxic concentration of paclitaxel (100 nmol/L) for 8 h did not cause any increase in cellular O_2^-. In contrast, paclitaxel caused a significant increase in extracellular O_2^- and H_2O_2 at 1 h (Fig. 1*B*). This H_2O_2 increase was detectable as early as 30 min (but not at 15 min) and continued to increase linearly up to 90 min. Addition of exogenous CuZnSOD further increased the extracellular H_2O_2 by 45% in the paclitaxel-treated cells, suggesting an increased conversion of O_2^- to H_2O_2 by the enzyme. SOD showed no effect on extracellular H_2O_2 when cells were not exposed to paclitaxel (data not shown). Because neither CuZnSOD nor O_2^- is able to pass cellular membranes, these data suggest that O_2^- production in the paclitaxel-treated cells was directly released outside the cells where it is subsequently dismutated into H_2O_2.

The ability of paclitaxel to induce elevation of extracellular H_2O_2 was also observed in a different human cell line HL-60 (Fig. 1*C*). Interestingly, using a subclone of HL-60 (C6F cells) completely defective in mitochondrial respiration (5), we showed that although the overall ROS generation was low due to respiration defect, paclitaxel caused a similar fold of increase in extracellular H_2O_2 in this cell culture (Fig. 1*C*). These data suggest that mitochondrial respiratory chain was not a significant source of paclitaxel-induced ROS generation, and that membrane-associated NOX would be the likely site of ROS production. These observations prompted us to further measure the activity of NOX in membrane fractions of MCF7 cells incubated with or without paclitaxel. As shown in Fig. 1*D*, exposure of MCF7 cells to 100 nmol/L paclitaxel induced a 2-fold increased in NOX activity, as evidenced by an *in vitro* luminescence assay. Similar results were obtained with human lung cancer H1299 cells (data not shown). Immunobloting showed that paclitaxel induced an increase in Rac1 protein (a positive regulator of NOX enzyme complex) in the membrane fraction of MCF7 cells (Fig. 1*D*), consistent with the activation of membrane-associated NOX.

Paclitaxel causes cytotoxic bystander effect mediated by H_2O_2. We speculated that the extracellular accumulation of ROS induced by paclitaxel might be toxic to bystander cells. To test this possibility, we first treated MCF7 cells with 100 nmol/L paclitaxel for 3 h and removed the drug by washing with fresh medium. A separate dish of MCF7 cells was prelabeled with a nontoxic green dye CMFDA (without paclitaxel) and then trypsinized for coculture with the washed MCF7 cells pretreated with paclitaxel (Fig. 2*A*). Adherent dead cells with compromised membrane integrity were revealed by directly staining with PI (red) in the culture dish. As shown in Fig. 2*B*, dead cells from the paclitaxel-treated population exhibited red fluorescent nuclear staining, whereas dead cells from the CMFDA-labeled bystander cells showed yellow nuclear staining due to colabeling with green (CMFDA) and red (PI) dyes. Quantitation of multiple samples showed that among the CMFDA-labeled bystander cells, the mean percentage of PI-labeled cells increased over 10-fold from 0.3% in the sample cocultured with control (untreated) cells to 3.6% in the sample cocultured with paclitaxel-treated cells (Fig. 2*C*; $P < 0.01$). It should be noted that this percentage probably underestimated the true percentage of dead cells because only the adherent cells were counted, and direct PI staining mainly revealed dead cells in the late stage. Nevertheless, among all

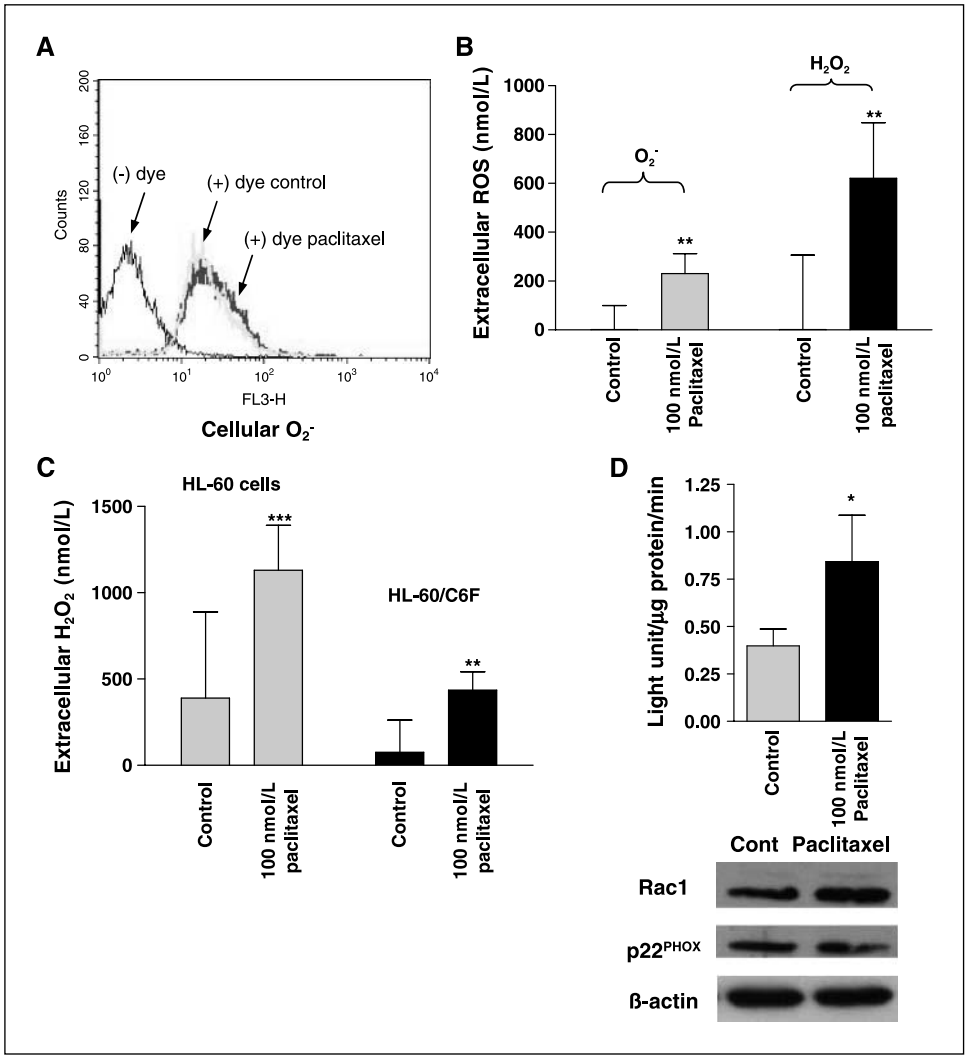

Figure 1. ROS production and NOX activity in cancer cells exposed to paclitaxel. *A,* intracellular level of superoxide in MCF7 cells exposed to 100 nmol/L paclitaxel for 8 h (*dark gray line*) and in control cells (*light gray line*) was assessed by cytometry using hydroethidine dye as previously described (5). *Black line,* spontaneous fluorescence in control cells without dye. *B,* extracellular concentrations of superoxide and hydrogen peroxide were measured in MCF7 cells incubated with or without paclitaxel for 1 h, as described in Materials and Methods. *Columns,* mean of two independent experiments carried out in quadruplicate; *bars,* SD. **, $P < 0.001$. *C,* extracellular concentration of H_2O_2 in HL-60 and HL-60/C6F cells incubated with or without paclitaxel for 1 h. ***, $P < 0.05$, difference between paclitaxel-treated and untreated cells. *D, top,* NOX activity and protein levels of Rac1, $p22^{phox}$, and β-actin in the membrane fractions of MCF7 cells treated with or without paclitaxel for 5 h. Lucigenin chemiluminescence assay was used to measure superoxide generation in the presence of NADPH as described in Materials and Methods. Light intensity was normalized to microgram protein per minute. *Columns,* mean of two independent experiments carried out in quadruplicate; *bars,* SD. *, $P < 10^{-6}$, difference between paclitaxel-treated and untreated cells. *Bottom,* 20 μg of membrane fraction proteins from paclitaxel-treated and untreated MCF7 cells were resolved by SDS-PAGE and blotted with specific antibodies.

PI-labeled cells (red + yellow), the percentage of yellow cells was 21 ± 7%, suggesting that a significant portion of cell death was due to the bystander effect.

To further investigate the role of ROS in mediating cytotoxic bystander effect, the paclitaxel-treated cells and the CMFDA-labeled cells were cocultured in the presence or absence of catalase or CuZnSOD in the culture medium. Catalase (2,000 units/mL), a specific scavenger of H_2O_2, effectively prevented the cytotoxic bystander effect, as evidenced by a significant decrease in percentage of cells with yellow nuclear staining among the CMFDA-labeled cells (Fig. 2*C*; $P = 0.003$). In contrast, addition of CuZnSOD (100 units/mL) to the coculture did not prevent the cytotoxic bystander effect. Instead, SOD caused a slight (but statistically insignificant) increase in cell death among the CMFDA-labeled bystander cells (Fig. 2*C*, compare *column 4* with *column 5*; $P = 0.3$). This slight increase likely reflected an increase of H_2O_2 in the medium due to conversion of superoxide to H_2O_2 catalyzed by SOD. Neither catalase nor SOD caused any significant change in the number of dead cells with red nuclear staining, indicating that neither enzyme was able to alter the direct cytotoxic effect of paclitaxel in MCF7 cells pretreated with the drug.

The ability of exogenous catalase in the culture medium to abolish the cytotoxic bystander effect strongly suggests that this effect was mediated by H_2O_2 and was not due to the possible presence of residual paclitaxel after washing.

Bystander cytotoxicity induced by microtubule-targeted agents. A different coculture method was then used to confirm the cytotoxic bystander effect of paclitaxel and to further evaluate other anticancer agents with different mechanisms of action. In this coculture system, the bystander cells were first labeled with ^{3}H-thymidine for two cell cycles (48 h) and washed free of unincorporated ^{3}H-thymidine before trypsinization for coculture with MCF7 cells pretreated with paclitaxel, vincristine, 5-FU, or doxorubicin. After 96 h of coculture, the radioactive DNA in the medium released from dead cells as a consequence of toxic bystander effect was quantified by liquid scintillation counting. As shown in Fig. 3*A*, the bystander toxic effect of paclitaxel was again observed, indicated by a significant increase of radioactivity released from the bystander cells. Interestingly, the microtubule destabilization agent vincristine also caused a substantial increase (32%) of radioactivity released from the bystander cells. Using the fluorescent double labeling coculture system described above, 300 nmol/L vincristine induced a significant increase of bystander

cells death with yellow nuclei (2.3 ± 0.6% in treated sample compared with 0.7 ± 0.1% in control, $P = 0.02$). We also tested various concentrations of paclitaxel (50–500 nmol/L) and taxotere (100–500 nmol/L) for the bystander cell killing activity and showed significant bystander effect in most concentrations tested (Fig. 3*B*). In contrast, a highly toxic concentration of 5-FU (1 mmol/L) or doxorubicin (3 μmol/L) did not cause cell death in the bystander cells detected by the radioactive assay (Fig. 3*A*), or by using CMFDA and PI double staining method (data not shown).

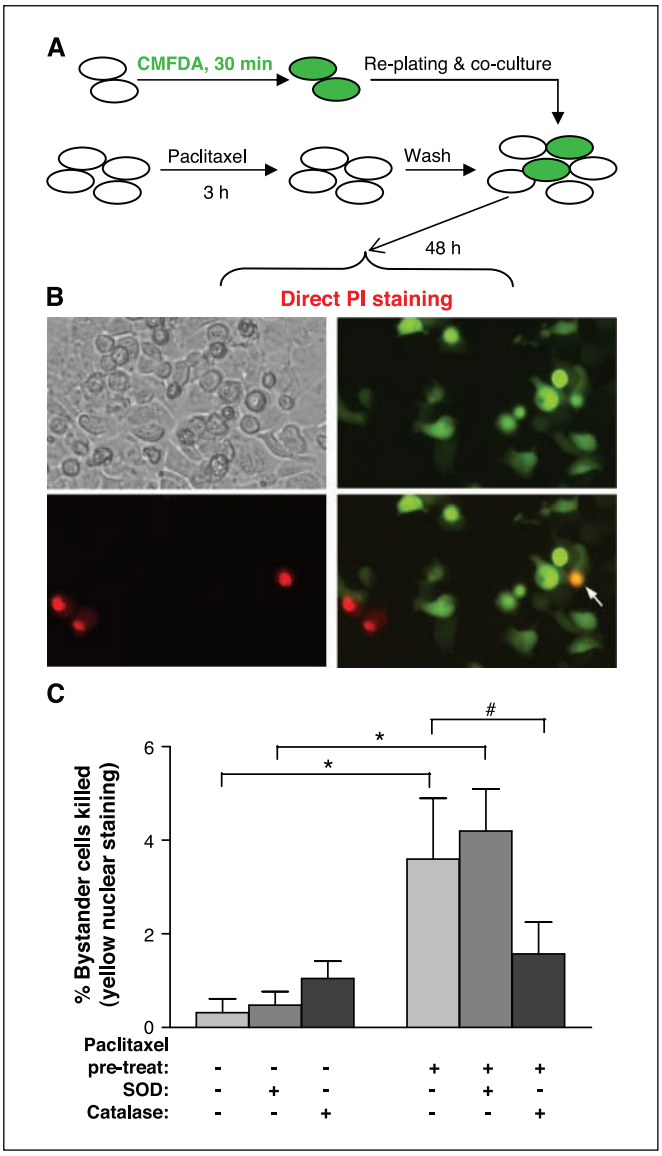

Figure 2. Induction of cell death by paclitaxel in neighboring untreated cells. *A,* experimental design used to assess the bystander effect of paclitaxel. MCF7 cells labeled with CMFDA were cocultured with MCF7 cells pretreated with or without 100 nmol/L paclitaxel for 3 h. Drug was removed by repeat washing before coculture. *B,* after 48 h of coculture, cell killing was evaluated by PI staining and examined under fluorescence microscopy (×40 objective) as described in Materials and Methods. Dead cells from the paclitaxel-treated population exhibited red fluorescent nuclear staining, whereas dead cells from the CMFDA-labeled bystander cells showed yellow nuclear staining (*arrow*). *C,* quantitation of cell killing in adherent CMFDA-labeled cells cocultured with control or paclitaxel-treated cells in the presence or absence of 100 units/mL CuZnSOD or 2,000 units/mL catalase as indicated. Cell death was expressed as the percentage of PI-labeled cells counted from multiple fields ($n = 9$). *Columns,* mean of three independent experiments carried out in triplicate; *bars,* SD. *, $P < 10^{-4}$; #, $P = 0.003$.

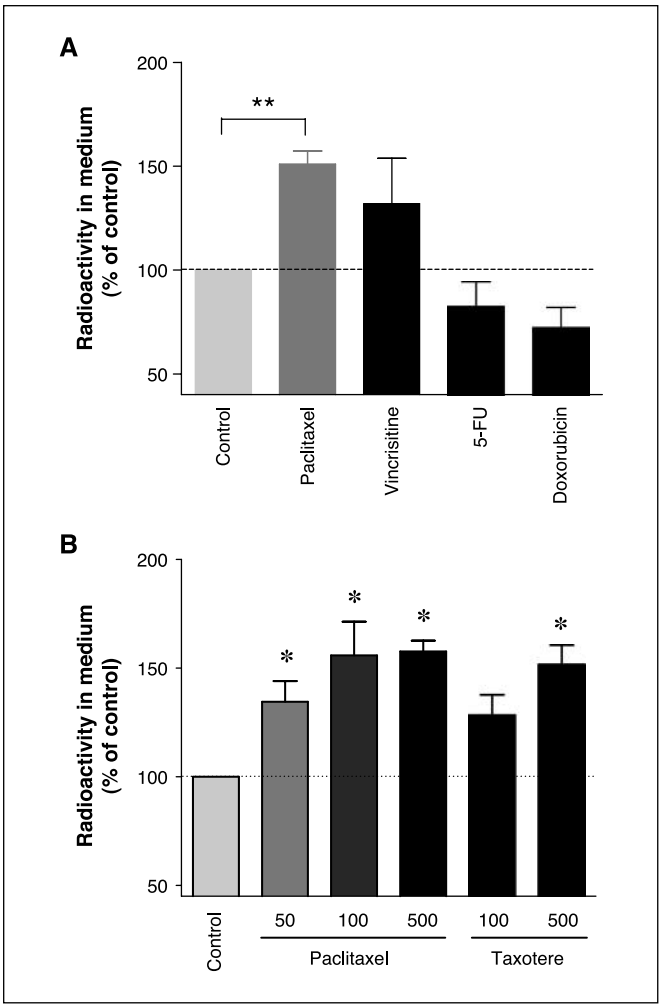

Figure 3. Bystander cytotoxicity induced by anticancer agents. *A,* MCF7 cells labeled with ^{3}H-thymidine were cocultured with MCF7 cells pretreated with or without 100 nmol/L paclitaxel, 300 nmol/L vincristine, 3 μmol/L doxorubicin, or 1 mmol/L 5-FU for 3 h as described in Materials and Methods. After 96 h, the level of radioactivity released in the culture medium was measured. Radioactivity levels are expressed as percentage of radioactivity compared with the control (^{3}H-thymidine–labeled cells cocultured with untreated cells). *Columns,* mean of three independent experiments; *bars,* SD. **, $P = 0.01$. *B,* bystander effects of various concentrations of paclitaxel and taxotere were measured by the radioactivity release assay in a similar fashion as in (*A*). *Columns,* mean of four experiments; *bars,* SD. *, $P = 0.05$.

Paclitaxel induces potent inhibition of bystander cell proliferation. Based on the observation that H_2O_2 released from the paclitaxel-treated cells was able to cause lethal damage to the bystander cells, we reasoned that it is possible that in addition to their severe toxic effect, the released ROS might also affect the proliferative capacity of the bystander cells. To test this possibility, the bystander cells were first labeled with CMFDA (green) and then cocultured with unlabeled MCF7 cells pretreated with or without paclitaxel in a similar fashion as described above. The density of the green cells (number of cells per mm^2) was then monitored over a 48-h period to evaluate their growing rate. As shown in Fig. 4*A*, the density of the green cells increased significantly 48 h after coculture with the control MCF7 cells, indicating that the CMFDA-labeled cells were viable and capable of proliferation, consistent with previous observation (12). Quantitation of multiple samples from separate culture wells

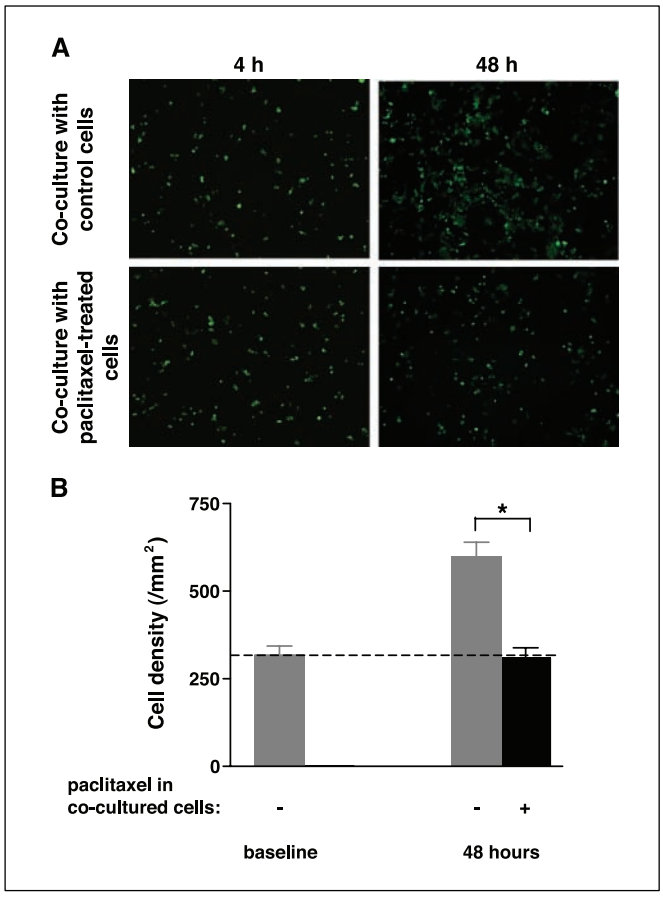

Figure 4. Antiproliferative bystander effect of paclitaxel. MCF7 cells labeled with CMFDA were cocultured with unlabeled MCF7 cells preincubated with or without 100 nmol/L paclitaxel for 3 h in a similar fashion as in Fig. 1. CMFDA-labeled cell density was evaluated 4 h after platting and 48 h after coculture, as described in Materials and Methods. *A,* representative photos of labeled cells cocultured with control or paclitaxel-treated cells (×10 magnification). *B,* quantitation of the bystander cell density in coculture. *Columns,* mean of three independent experiments carried out in triplicate; *bars,* SD. *, $P < 10^{-4}$.

showed that the green cell density increased from 317 ± 26 to 598 ± 42 cells per mm^2 at 48 h after seeding to the coculture dish containing control (untreated) MCF7 cells (Fig. 4*B*). Importantly, when the green cells were coculture with MCF7 cells pretreated with 100 nmol/L paclitaxel for 3 h (drug was removed by washing with fresh medium before coculture), the proliferation of these bystander cells was almost completely inhibited (Fig. 4*A* and *B*). Similar results were obtained using the human lung cancer H1299 cells (data not shown). Thus, paclitaxel was able to induce a potent inhibition on proliferation of the bystander cells. These results were consistent with previous observations that exposure of cancer cells to H_2O_2 suppresses cell proliferation and induces cell death, even at micromolar concentration (14).

Several anticancer agents, such as arsenic trioxide, doxorubicin, bleomycin, cisplatin, 5-FU, and paclitaxel, have been shown to induce ROS generation in cancer cells (15, 16). Various mechanisms have been described, including respiratory chain disruption, redox cycling, or p53-mediated mitochondrial oxidase activation (5, 15, 16). To date, the mechanism responsible for ROS induction by paclitaxel remains elusive. Our study showed that at a clinically relevant concentration, paclitaxel is able to activate the membrane-associated NOX, leading to extracellular release of O_2^-, which is subsequently converted to H_2O_2 (spontaneous and/or SOD catalyzed). Plasma membrane–associated NOX is the main source of extracellular O_2^- and also seems to be the main source of ROS production induced by paclitaxel. The ability of paclitaxel to cause ROS generation in the mitochondrial respiration-defective cells (HL-60/C6F clone) suggests that mitochondria respiratory chain is not the site where paclitaxel induces ROS production. The observation that paclitaxel treatment was followed by an increased translocation of Rac1 to the membrane fraction, a crucial step in active NOX assembling (7), further suggests that activation of NOX may be a key mechanism of action. This result is in line with previous report showing that microtubules play a key role in Rac1 transport, and that the polymerization state of microtubules affects the Rac1 location to the membranes (17). It is possible that the disturbance of microtubule polymerization by paclitaxel, taxotere, or vincristine render Rac1 stabilized in the active NOX complex, leading to increased ROS generation. Interestingly, we observed that higher concentrations of paclitaxel did not proportionally cause further increase in ROS generation (data not shown), suggesting that the drug-induced disturbance of microtubule polymerization state enhanced ROS production due to stabilization of active NOX, which could not be further activated by higher drug concentrations. This may also explain why the elevated bystander cell killing effect was not linearly concentration dependent (Fig. 3*B*).

Although the bystander effect of ionizing radiation has been well described (18), there are few reports of such effect with chemotherapy agent. By using two different methods, we showed that paclitaxel displayed cytotoxic bystander effect in neighboring cancer cells. By comparing the number of dead cells with yellow or red nuclear staining, we estimated that about 20% of cell death occurred in the bystander cells. Because the ratio of paclitaxel-treated cells and bystander cells in the coculture was 3:1 (25% bystander cells), it seemed that paclitaxel killed nearly the same proportion of cells in the population directly exposed to the drug and in those submitted to bystander effect under our experimental conditions. In addition, paclitaxel was able to almost completely inhibit the proliferation of the bystander cells. Taken together, these data suggested that the bystander effects, both lethal damage and inhibition of proliferation, may play a significant role in the antitumor activity of paclitaxel. It is worth noting that paclitaxel, like most anticancer drugs, has limited ability to reach tumor cells that are distant from blood vessels (19). Because H_2O_2 can diffuse relatively far from its production origin, it may act on cells that are not reached by paclitaxel. It was recently reported that SOD mimics that increase H_2O_2 production are able to increase the antitumor activity of paclitaxel (4, 14). Our findings that NOX activation by paclitaxel leads to bystander effects against cancer cells open new perspectives to improve the therapeutic activity of paclitaxel and potentially other microtubule-targeted agents.

Acknowledgments

Received 10/21/2006; revised 1/24/2007; accepted 3/2/2007.

Grant support: Lilly Foundation and a Rosalie B. Hite Fellowship from the Graduate School of Biomedical Sciences, University of Texas Health Sciences Center at Houston and University of Texas M. D. Anderson Cancer Center.

The costs of publication of this article were defrayed in part by the payment of page charges. This article must therefore be hereby marked *advertisement* in accordance with 18 U.S.C. Section 1734 solely to indicate this fact.

References

1. Honore S, Pasquier E, Braguer D. Understanding microtubule dynamics for improved cancer therapy. Cell Mol Life Sci 2005;62:3039–56.
2. Alexandre J, Batteux F, Nicco C, et al. Accumulation of hydrogen peroxide is an early and crucial step for paclitaxel-induced cancer cell death both *in vitro* and *in vivo*. Int J Cancer 2006;119:41–8.
3. Ramanathan B, Jan KY, Chen CH, Hour TC, Yu HJ, Pu YS. Resistance to paclitaxel is proportional to cellular total antioxidant capacity. Cancer Res 2005; 65:8455–60.
4. Alexandre J, Nicco C, Chereau C, et al. Improvement of the therapeutic index of anticancer drugs by the superoxide dismutase mimic mangafodipir. J Natl Cancer Inst 2006;98:236–44.
5. Pelicano H, Feng L, Zhou Y, et al. Inhibition of mitochondrial respiration: a novel strategy to enhance drug-induced apoptosis in human leukemia cells by a reactive oxygen species-mediated mechanism. J Biol Chem 2003;278:37832–9.
6. Lambeth JD. NOX enzymes and the biology of reactive oxygen. Nat Rev Immunol 2004;4:181–9.
7. Cheng G, Diebold BA, Hughes Y, Lambeth JD. Nox1-dependent reactive oxygen generation is regulated by Rac1. J Biol Chem 2006;281:17718–26.
8. Teufelhofer O, Weiss RM, Parzefall W, et al. Promyelocytic HL60 cells express NADPH oxidase and are excellent targets in a rapid spectrophotometric microplate assay for extracellular superoxide. Toxicol Sci 2003; 76:376–83.
9. Zhou M, Diwu Z, Panchuk-Voloshina N, Haugland RP. A stable nonfluorescent derivative of resorufin for the fluorometric determination of trace hydrogen peroxide: applications in detecting the activity of phagocyte NADPH oxidase and other oxidases. Anal Biochem 1997;253:162–8.
10. Mohazzab KM, Wolin MS. Sites of superoxide anion production detected by lucigenin in calf pulmonary artery smooth muscle. Am J Physiol 1994;267:L815–22.
11. Sorescu D, Somers MJ, Lassegue B, Grant S, Harrison DG, Griendling KK. Electron spin resonance characterization of the NAD(P)H oxidase in vascular smooth muscle cells. Free Radic Biol Med 2001;30:603–12.
12. Burch MG, Pepe GJ, Dobrian AD, Lattanzio FA, Jr., Albrecht ED. Development of a coculture system and use of confocal laser fluorescent microscopy to study human microvascular endothelial cell and mural cell interaction. Microvasc Res 2005;70:43–52.
13. Stoitzner P, Tripp CH, Eberhart A, et al. Langerhans cells cross-present antigen derived from skin. Proc Natl Acad Sci U S A 2006;103:7783–8.
14. Laurent A, Nicco C, Chéreau C, et al. Controlling tumor growth by modulating endogenous production of reactive oxygen species. Cancer Res 2005;65:948–56.
15. Pelicano H, Carney D, Huang P. ROS stress in cancer cells and therapeutic implications. Drug Resist Updat 2004;7:97–110.
16. Hwang PM, Bunz F, Yu J, Rago C, et al. Ferredoxin reductase affects p53-dependent, 5-fluorouracil-induced apoptosis in colorectal cancer cells. Nat Med 2001;7: 1111–7.
17. Zuo L, Ushio-Fukai M, Hilenski LL, Alexander RW. Microtubules regulate angiotensin II type 1 receptor and Rac1 localization in caveolae/lipid rafts: role in redox signaling. Arterioscler Thromb Vasc Biol 2004;24: 1223–8.
18. Azzam EI, de Toledo SM, Little JB. Oxidative metabolism, gap junctions and the ionizing radiation-induced bystander effect. Oncogene 2003;22:7050–7.
19. Tannock IF, Lee CM, Tunggal JK, Cowan DS, Egorin MJ. Limited penetration of anticancer drugs through tumor tissue: a potential cause of resistance of solid tumors to chemotherapy. Clin Cancer Res 2002;8:878–84.